Fireball@LNF - Letter of Intent

E. E. Los[1], G. Gregori[1], A. Dyson[1], B. T. Huffman[1], H. Ramm[1], B.-K. Tan[1], S. Sarkar[1], S. Zhang[1], D. A. Uzdensky[1], V. Stergiou[1, 2], P. Alexaki[2], N. Charitonidis[2], A. Goillot[2], C. D. Arrowsmith[3], D. H. Froula[3], A. R. Bell[4], R. Bingham[4,5], J. W. D. Halliday[4], R. M. G. M. Trines[4], A. Phelps[5], K. Ronald[5], D. Speirs[5], P. J. Bilbao[6], F. D. Cruz[6], L. O. Silva[6], M. P. Anania[7], M. Bazzi[7], B. Buonomo[7], S. Cantarella[7], F. Cardelli[7], F. Chiarelli[7], A. Clozza[7], C. Curceanu[7], E. Diociaiuti[7], R. Donghia[7], L. G. Foggetta[7], D. Di Giovenale[7], C. Di Giulio[7], E. Di Pasquale[7], A. Ghigo[7], A. Liedl[7], S. Manti[7], F. Napolitano[7], A. Scordo[7], F. Sgaramella[7], F. Sirghi[7], C. Taruggi[7], A. Trigilio[7], A. Vannozzi[7], J. T. Gudmundsson[8,9], B. Reville[10], T. Vieu[10], C. P. Ridgers[11], P. Simon[12], A. G. R. Thomas[13], L. Willingdale[13], E. D. O. Wilhelmi[14], L. Serafini[15], V. Petrillo[15], and R.A.C. Cairns[16]

[1]Department of Physics, University of Oxford, Parks Road, Oxford, OX1 3PU, UK
[2]European Organization for Nuclear Research (CERN), CH-1211, Geneva 23, Switzerland
[3]University of Rochester Laboratory for Laser Energetics, Rochester, NY, 14623, USA
[4]STFC Rutherford Appleton Laboratory, Chilton, Didcot, OX11 0QX, UK
[5]Department of Physics, University of Strathclyde, Glasgow, G4 0NG, UK
[6]GoLP/Instituto de Plasmas e Fusão Nuclear, Instituto Superior Técnico, Universidade de Lisboa, 1049-001, Lisboa, Portugal
[7]Laboratori Nazionali di Frascati, Istituto Nazionale Fisica Nucleare, Frascati, Italy
[8]Science Institute, University of Iceland, Dunhaga 3, IS-107, Reykjavik, Iceland
[9]Division of Space and Plasma Physics, School of Electrical Engineering and Computer Science, KTH Royal Institute of Technology, SE-100 44, Stockholm, Sweden
[10]Max-Planck-Institut für Kernphysik, Saupfercheckweg 1, D-69117, Heidelberg, Germany
[11]Department of Physics, York Plasma Institute, University of York, York, YO10 5DD, UK
[12]GSI Helmholtzzentrum für Schwerionenforschung GmbH, Planckstraße 1, 64291, Darmstadt, Germany
[13]The Gérard Mourou Center for Ultrafast Optical Science, University of Michigan, Ann Arbor, Michigan 48109, USA
[14]Deutsches Elektronen Synchrotron DESY, D-15738 Zeuthen, Germany
[15]INFN Sez. Milano and Universita' degli Studi di Milano, Dipartimento di Fisica, Via Celoria 16, 20133 Milano, Italy
[16]School of Mathematics and Statistics, University of St Andrews, St Andrews, Fife, KY16 9SS, UK

November 13, 2024

Abstract

Gamma Ray Bursts (GRBs) are the brightest radiation sources in the known Universe. However, the mechanisms responsible for such bright emissions are not well-understood. The fireball model of GRB invokes the presence of large-scale magnetic fields and predict a complex interplays between fields, plasmas and energetic particle to explain the spectra and temporal profiles of the observed GRB emission. In many cases, observations of GRBs and Fast Radio Bursts (FRBs) – enigmatic transient emitters – suggest that the source brightness and hence temperatures are at odds with currents models of synchrotron absorption and inverse Compton scattering. A coherent radiation process, such as maser emission by leptons in a tapered magnetic field, may explain these observations. Here we outline a three-stage experimental program. In the first campaign, the instabilities which perturb an electron-positron beam in a background plasma will be studied in conditions relevant to astrophysical environments. In the second stage, we will study the interaction of electron and positron beams in the presence of a tapered magnetic field to generate maser emission. And in the third campaign we will look at the processes leading to the generation of collisionless

shocks and particle acceleration. These campaigns will provide much-needed insights into the physical processes which underpin GRB, FRB, and cosmic-ray generation, allowing the validity of current models to be investigated and supplementing efforts to model these processes computationally.

1 Scientific Case

To explain observations of gamma-ray bursts (GRBs), fast radio bursts (FRBs), and cosmic-ray acceleration, it is essential to understand the complex interplay between processes involving relativistic particle beams, plasma instabilities, magnetic fields, and radiation production. However, telescopes can not resolve the microphysical processes at play, and the range of length scales needed to model the interplay of macro- and micro-scale processes computationally requires extremely expensive simulations. We propose three experimental campaigns to investigate the processes which underpin GRB generation and particle acceleration in regimes relevant to astrophysical environments. The first campaign will study the instabilities which modulate an electron-positron pair beam propagating through an under-dense plasma and their associated magnetic fields. The second campaign will study the behaviour of electron and positron beams in a tapered magnetic field. The third campaign will investigate shock generation and its implications for particle acceleration. The beam test facility (BTF) provides unique energetic electron and positron beams that can be used to test these processes independently. Moreover, by generating pair showers with converter foils neutral pair beams can also be produced, thus providing a close equivalent to astrophysical GRBs.

1.1 Gamma ray bursts

Pair production is a ubiquitous process in pulsar, magnetar and black hole magnetospheres. Gamma ray bursts (GRBs), the most luminous transients in the universe, are produced in those environments, and during supernova events which precede the formation of such compact objects. It has been proposed that the processes which produce GRBs may also accelerate cosmic rays to extremely high energies up to $10^{20}\,\mathrm{eV}$ [1]. However, the mechanisms which are responsible for the production and propagation of GRBs and highly energetic cosmic rays are not well understood. Fireballs are highly energetic, optically thick jets of electron-positron pairs with some hadronic contamination [2]. One of the leading models of GRB generation, the fireball model, proposes that some characteristic features of GRB spectra are consistent with synchrotron radiation generated during the interaction of a fireball with magnetic fields generated by instabilities (e.g., Weibel or filamentation) which arise when the pair beam propagates through an underdense background plasma. If the magnetic field is sufficiently strong, it can drive a relativistic shock in this background plasma. Density pertubations upstream of the shock generate turbulence downstream of the shock which can amplify the magnetic field [3], thus enhancing synchrotron emission.

A second, competing GRB model, the cannonball model, proposes that GRBs are generated by relativistic blobs of plasma, ejected from compact astrophysical objects, which undergo inverse Compton scattering from ambient photons in the supernova glory [4]. The relative validity of the fireball and cannonball models is the subject of considerable interest and debate.

1.2 Maser emission

The high fluxes and great distances of GRB and FRB sources from Earth suggest that their intrinsic source brightness temperatures exceed the maximum temperatures achievable due to inverse Compton scattering, which induces rapid cooling once this threshold ($\sim 10^{12}\,\mathrm{K}$) is surpassed [5]. Some observed characteristics of FRBs, including their extremely high source brightness, high degree of polarisation and spectral and temporal structure [6] may be explained by a coherent radiation mechanism. One promising candidate is cyclotron maser emission, predicted to occur when a lepton beam propagates into a magnetic mirror (a converging magnetic field geometry). As this happens, the lepton beam undergoes a population inversion in transverse momentum (the number of leptons with higher transverse momenta exceeds those with lower transverse momenta), due to energy and momentum conservation [7]. As the beam interacts with the magnetic field, it de-excites, emitting coherent synchrotron radiation, or maser emission [8].

Maser radiation has been observed for non-relativistic pairs [9, 10]. However, relativistic effects, which are predicted to have a significant impact on the cyclotron resonance condition and spectra of emitted radiation, have not yet been seen. We aim to study the spectrum, power and polarisation of maser radiation produced by pair beams in order to gain insight into such emission generated by relativistic pairs and elucidate unexplained FRB observations.

1.3 Particle Acceleration

Due to their relativistic motion and the large energy content carried by the leptons, GRBs are believed to be unique sites of particle acceleration, particularly for the ultra-energetic extragalactic cosmic rays observed on Earth [11]. Particles crossing a relativistic shock boundary undergo first-order Fermi acceleration, experiencing an increase in energy by $\Gamma_{\rm rel}^2$ for the first boundary crossing, where $\Gamma_{\rm rel}$ is the relative Lorentz factor between the plasma flows upstream and downstream of the shock [12]. Particles may be also be accelerated stochastically when reflected by regions of counter-propagating magnetised plasma, relative to the particle rest frame, an effect known as second-order Fermi acceleration.

For example, numerical simulations show that while relativistic collisionless shocks are associated with efficient particle acceleration when propagating into a magnetized and homogeneous media; as the magnetization increases, particle acceleration becomes suppressed. This process is reversed if the upstream plasma carries kinetic-scale inhomogeneities, as is often the case in astrophysical environments [13]. There is no clear observational evidence of any of these processes happening in GRBs, and experimental validation is needed. The problem is that the feedback loop of particle beams driving the magnetic field growth in the background plasma, and the corresponding role of the amplified magnetic field in energizing cosmic rays to high energies is a complex, non-linear, multiscale problem. Computer simulations provide invaluable insights into how particle transport and acceleration occur, but they are limited by the spatial and temporal range and resolution scales they can achieve even with the largest supercomputer facilities, hence we are forced to resort to a variety of simplified models.

Since the beam Lorentz factor and the beam-plasma density ratio ($n_{\rm b}/n_{\rm p}$) are comparable for both laboratory and astrophysical GRB systems, there is a complete analogy between the laboratory beams and GRBs in terms of microscopic beam instabilities (even if the macroscopic physical conditions are rather different). Our proposed laboratory experiments can however access the late-time evolution of the plasma instabilities, and thus both validate and complement numerical predictions.

2 Suitability of BTF

At HiRadMat (CERN) we were able to perform initial experiments to validate the viability of the work that we want to perform at the BTF facility [14]. There, we obtained the first experimental results confirming the generation of high-density, quasi-neutral, relativistic electron-positron pair beams using the 440 GeV/c beam at CERN's Super Proton Synchrotron (SPS) accelerator. Monte Carlo simulations agree well with the experimental data and show that the characteristic scales necessary for collective plasma behaviour, such as the Debye length and the collisionless skin depth, are exceeded by the measured size of the produced pair beams. The particle number we expect to achieve at BTF is comparable (albeit lower in density) to what is possible at HiRadMat, but with the following key differences, which demonstrate that BTF is uniquely suited for the planned experimental campaigns:

- At BTF electron positron pairs are produced via an electromagnetic shower, removing additional contaminants such as pions and muons – those particles constitute up to a few percents of the HiRadMat beam. In addition, there are no remaining primary protons as is the case at HiRadMat. The presence of energetic, charged hadrons in the beam provides a seed magnetic field which affects instability onset and the subsequent evolution of the pair beam spatial structure. At BTF, we will be able to study the beam instabilities without these effects.

- An important advantage of BTF is a possibility of having electron and positron beams directly from the accelerator, without the need of using a converter foil. We plan to use this facility in order to test maser emission by singly charged (nearly monoenergetic) beams. Such a mode of operation is not feasible at HiRadMat.

- BTF offers simultaneous access to a laser and a lepton beam. This offers an opportunity to explore magnetic field amplification via the turbulent dynamo effect using a laser-solid target interactions mm-scale high-density plasma region. This will boost our ability to drive relativistic shocks in the background plasma.

- The minimal on-axis hadron component at BTF permits the placement of on-axis photon detectors, once the lepton beam has been directed off-axis using dipole magnets. This allows gamma-rays generated via inverse Compton scattering to be measured.

- The BTF experiment is complementary to the experiment at CERN in terms of scheduling – CERN is expected to start the long shutdown in mid-2026, in line with the estimated start of the BTF experiment. This would allow us to continue this research without interruption.

Finally, the HiRadMat experiment, as well as extensive testing performed in Oxford, have provided us with adequate expertise in the deployment of the plasma cell we plan to use in the BTF experiment [15].

3 Description of the Proposed BTF Experiment

In the following section, the campaigns which will investigate maser emission, pair beam instabilities and particle acceleration in magnetic fields are discussed under three work packages (WPs).

3.1 E1: Pair beam instability study

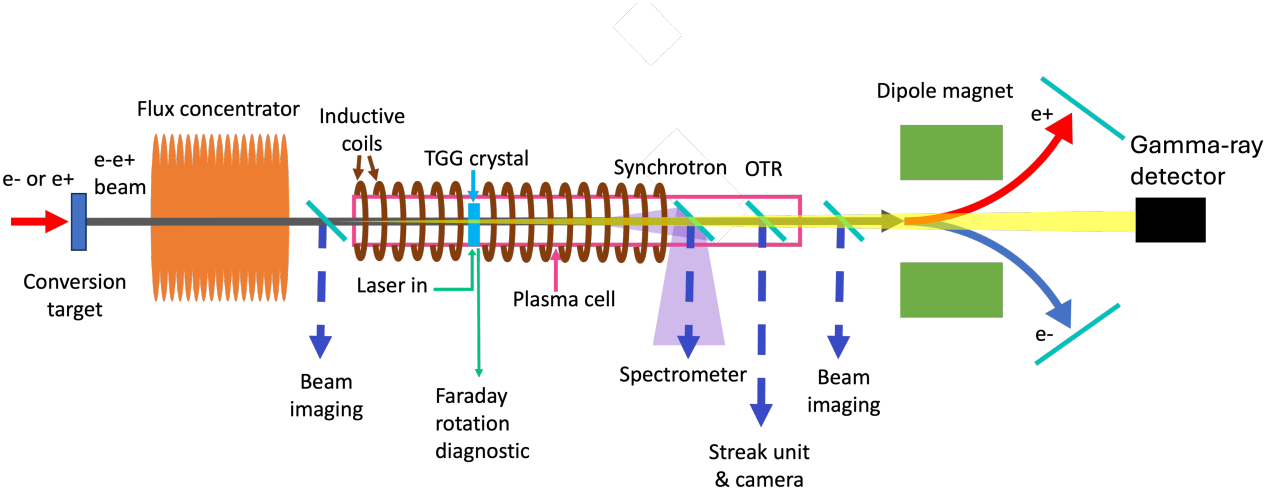

Figure 1: A 0.5 GeV lepton beam incident on a tantalum conversion target generates a cascade of electron-positron pairs. The pairs are collimated by the flux concentrator before entering the plasma cell. A radio-frequency inductively-coupled discharge ionises the plasma, producing plasma densities up to $10^{14}\,\mathrm{cm}^{-3}$. The magnetic fields generated as the beam becomes unstable in the plasma are measured using the Faraday rotation of an optical laser in a terbium gallium garnet (TGG) crystal suspended in the plasma. A thin pellicle coupled to a spectrometer will measure the spectrum of synchrotron emission. The longitudinal profile of the pair beam will be measured by streaking optical transition radiation generated as the pair beam passes through a conducting foil. The transverse profile and spectrum of the pair beam will be measured with luminescent screens placed before and after the cell and a magnetic spectrometer. X-rays and gamma-rays, produced by inverse Compton scattering of optical plasma emission from the pair beam, will be measured by an on-axis calorimeter.

In WP1, we aim to study the instabilities which perturb the pair beam and result in magnetic field generation. In particular, by measuring the growth rates of these instabilities and the magnetic field strength at saturation, we can infer the above for fireballs emitted by blazars, magnetars and neutron stars using appropriate scaling laws. We will also measure the power, spectrum and polarisation of synchrotron radiation generated as the pairs interact with self-generated magnetic fields.

In the experimental setup, illustrated in fig. 1, a lepton beam interacting with a high-Z target generates bremsstrahlung which produces electron-positron pairs via the Breit-Wheeler process.

Preliminary studies of pair yield, shown in figure 2, conducted using FLUKA, indicate that pair beam densities, n_b, of $10^8\,\mathrm{cm}^{-3}$ - $10^9\,\mathrm{cm}^{-3}$ with an electron:positron ratio of 40:60 are achievable for a $1\,\mathrm{cm}^2$ electron beam of 1 ns duration. With further optimizations (different materials and thicknesses), we believe a 50:50 ratio is within reach (to be confirmed with further FLUKA simulations).

As the pair beam propagates through the plasma, optical plasma photons will scatter from the pair beam (inverse Compton scattering) and experience an upshift in energy proportional to γ^2, where γ is the lepton beam Lorentz factor. An on-axis photon calorimeter will be used to retrieve the scattered photon power and spectrum, which will lie in the MeV range. This measurement will serve as an upper estimate of the radiated power for the cannonball model of GRBs. A comparison of the synchrotron and Compton emission will shed light on the relative validity of the fireball and cannonball models of GRBs.

A radio frequency inductively-coupled Ar plasma discharge in a 3 m long cell driven by a 6 kW power source, will achieve plasma densities, n_p, up to $10^{14}\,\mathrm{cm}^{-3}$, at which shock formation is possible. At these densities, the collisionless skin-depth of the plasma is 20 times smaller than the $1\,\mathrm{cm}^2$ pair beam. We obtain linear growth rates for the oblique and current filamentation instabilities of $0.18\,\mathrm{ns}^{-1}$ ($\approx$ 2 e-folding lengths) and $1.2\,\mathrm{ns}^{-1}$ ($\approx$ 12 e-folding lengths), respectively, for a 0.1 GeV pair beam with $n_b = 10^9\,\mathrm{cm}^{-3}$ with 25 mrad momentum

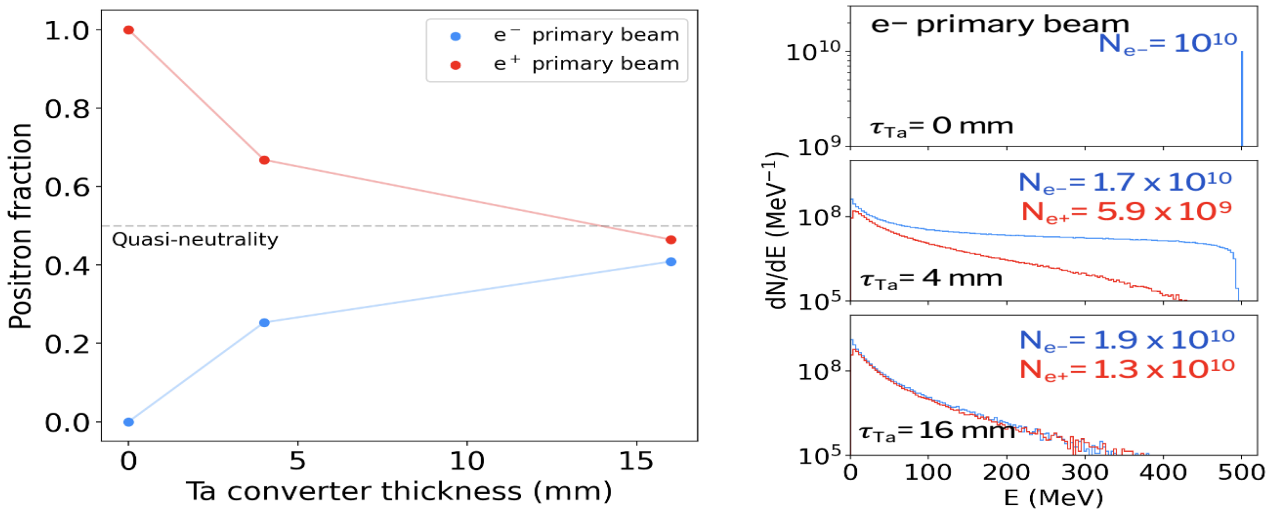

Figure 2: FLUKA simulations of pair spectra generated when an electron beam (top right) interacts with 4 mm (middle right) and 16 mm (bottom right) thick Ta targets. The beam neutrality is shown as a function of target thickness (left).

spread, propagating though a $2 \times 10^{12}\,\mathrm{cm}^{-3}$ density plasma. At our previous campaign at CERN, magnetic fields $\sim 1\,\mathrm{mT}$ were measured. Pairs interacting with the magnetic fields will produce broadband synchrotron radiation with peak intensity in the visible spectrum.

This campaign does not require a flux-concentrator, but we will use it to control the pair beam collimation if it becomes available. If the flux-concentrator is to be built by LNF we estimate it would take about two years of work (see Gantt chart below), but we are also investigating the possibility of procuring it via a collaboration with the Paul Scherrer Institute [16].

The plasma instabilities, magnetic fields, synchrotron emission and Compton scattered photons will be measured using a suite of diagnostics, as discussed below.

3.1.1 Faraday rotation

A probe laser with $\lambda = 532\,\mathrm{nm}$ passes through a linear polariser and a beamsplitter. The reflected signal acts as a reference, while the transmitted signal passes through the TGG crystal which is suspended in the plasma. Upon exiting the crystal, the probe beam is passed through a second linear polariser and compared to the reference signal. The change in polarisation is extracted from the difference in intensity of the probe and reference signals. The resulting signal is measured using a photodiode coupled to a fast oscilloscope with sub-ns temporal resolution. This diagnostic has been fielded successfully on a previous campaign at CERN.

3.1.2 Pair spectrometer

A dipole electromagnet placed after the flux concentrator will disperse the electrons or positrons onto a set of scintillation screens either side of the beam axis. This maps the energy of each lepton to a position along the screen, which is then used to retrieve the lepton spectrum. The vertical axis along the screen indicates the beam divergence.

3.1.3 Luminescent screens

Two luminescent screens before and after the flux converter will measure the transverse profile of the lepton beam, allowing the development of the population inversion in transverse momentum to be monitored.

3.1.4 Synchrotron radiation

A measurement of the spectrum and polarisation of the synchrotron radiation would complement the Faraday rotation diagnostic, providing additional information regarding the structure, scale and orientation of the magnetic fields generated by plasma instabilities.

We will use a thin pellicle with a non-conductive reflective coating to reflect the synchrotron emission without perturbing the pair beam. The non-conductive coating minimises background optical transition radiation (OTR) generated as the pair beam passes through the pellicle. An imaging line or optical fibre bundle will be used to transport the synchrotron radiation to a gated spectrometer. We will have the option of driving two

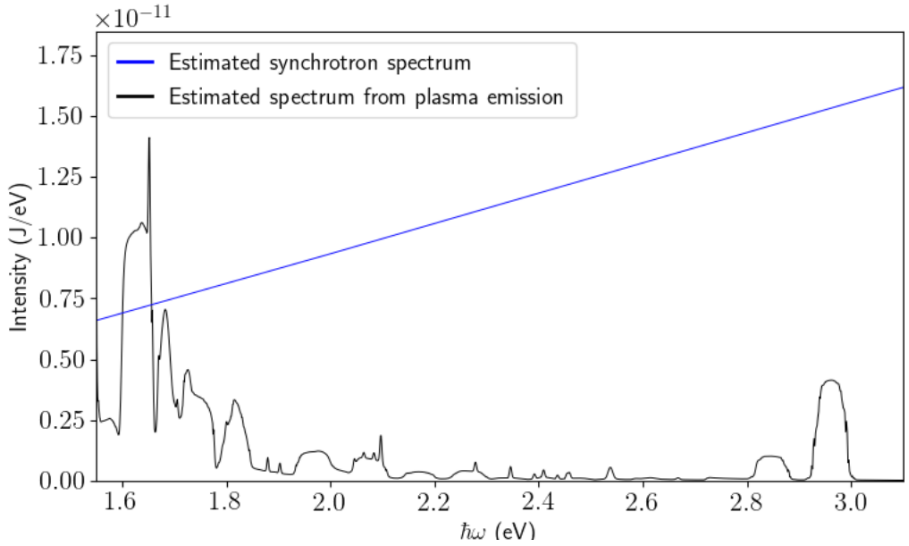

Figure 3: PIC simulations of the synchrotron emission for visible wavelengths ($\lambda = 400 - 800$nm), compared to the plasma emission simulated using the PrismSPECT collisional-radiative spectral analysis code. The emission is integrated over 2 ns, the exposure time of the gated spectrometer we plan to field.

orthogonally-oriented polarisation-dependent birefringent crystal into the signal path before the spectrometer to measure the signal polarisation. We will use a 2 ns gated spectrometer to reduce optical emission from the plasma, the primary source of background for this diagnostic. Additional sources of background may include scintillation light from pairs interacting with the optical fibres, Cherenkov emission from the beam travelling through the plasma, and OTR generated by the beam passing through the plasma cell windows. Background emission at wavelengths outside of the range of interest may be removed using band-pass filters. Sources of background in the optical range can be subtracted from the signal by taking reference shots with the beam and without the plasma. The background due to plasma emission can be subtracted from the signal by taking reference images with the plasma discharge emission, without the beam.

3.1.5 Inverse Compton scattering

Since the beam Lorentz factor and the beam-plasma density ratio are comparable for both laboratory and astrophysical GRB systems, there is a complete analogy between the laboratory beams and GRBs in terms of microscopic beam instabilities (even if the macroscopic physical conditions are rather different). This is important as several studies have found the "vanilla" synchrotron model to be inconsistent with observations [17]. Moreover, inverse Compton scattering (ICS) of the optical photon background of the plasma cell (E_{opt}) produces emission $E_{ICS} \sim 2\gamma^2 E_{opt} \sim 0.5$–2 MeV. As this emission is in a very different energy band than the synchrotron spectrum, the experiment provides a way to discriminate between two processes and verify predictions from the Fireball *vs* the Cannonball models [4]. However, since the optical depth for inverse Comptonization is $\ll 1$ in the laboratory – the emission from the laboratory jets will therefore not be representative of the emission coming from optically thick astrophysical GRBs.

We plan to commission a multi-KeV to MeV photon spectrometer to directly measure the ICS emission from the pair beam. The details of this spectrometer are currently under discussion with the INFN team in Frascati (Dr Catalina Curceanu), but it is within our expertise and capabilities for the full implementation in the experiment.

3.1.6 Time-resolved optical transition radiation

The longitudinal structure of the pair beam will be diagnosed by streaking OTR generated by the pair beam as it passes through a conducting foil. The OTR emitted from the front surface of the screen will be collected and transported to an optical streak camera with 5 ps resolution at 11 ns sweep time (i.e., temporal window) allowing longitudinal modulations in the beam on the order of the skin depth (0.5 mm for plasma densities of $10^{14}\,\mathrm{cm}^{-2}$, corresponding to a time period of 11 ps) to be resolved. This will be crucial for understanding the development of longitudinal instabilities, in particular their growth, saturation and competition with transverse instabilities.

Reference data taken without the plasma will be used to distinguish between beam micro-bunching and longitudinal structure induced by plasma instabilities.

3.2 E2: Maser emission

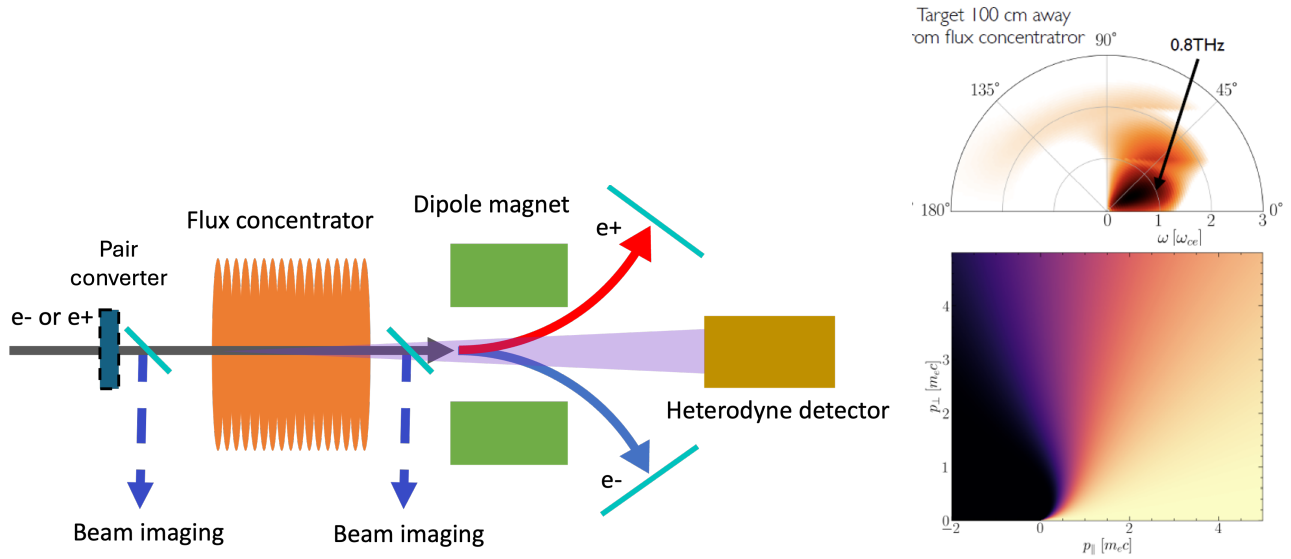

Figure 4: Left: Experimental set-up for maser emission measurement. A 0.1-0.5 GeV electron or positron beam with 2-4 nC charge emits maser radiation at sub-mm wavelengths as it propagates through the flux concentrator. A Ta converter target can be placed in the lepton beam to produce a neutral pair beam. The maser emission will be measured using a heterodyne mixer. Luminescent screens before and after the flux concentrator will measure the transverse beam distribution. Subsequently, a dipole electromagnet will disperse the electron or positron beam onto one of two luminescent screens either side of the beam axis, enabling spectral retrieval. Bottom right: a pair beam propagating through a tapered magnetic field (generated by the flux concentrator) develops a "horseshoe" distribution in transverse momentum due to conservation of energy and magnetic momentum. Top right: the angular distribution of maser emission radiated by a pair beam generated by a lepton beam in a Ta target placed 100 cm upstream from the flux concentrator.

In the second phase of the experimental campaign, we will investigate whether the high brightness and degree of polarisation of FRBs is consistent with maser emission. We will probe the maser instability driven by electron and positron beams interacting with a longitudinally tapered magnetic field, generated using a flux concentrator, comprised of electromagnets with bespoke geometries and strengths. Simulations will be used to inform the geometry and placement of the electromagnet to optimise the maser yield. The polarisation and spectrum of maser emission will be measured using a heterodyne detector. The lepton beam transverse profile and spectrum will be measured using luminescence screens and a magnetic spectrometer.

3.2.1 Particle spectrometer

The electron and positron spectra will be measured using the dispersive magnetic spectrometer fielded in E1. This diagnostic will diagnose the pair spectra produced when the lepton beam collides with a tantalum target, and will serve as the primary diagnostic for first-order Fermi acceleration, which would result in high numbers of higher-energy pairs on the spectrometer, and second-order Fermi acceleration, which would reduce the number of measured pairs due to reflection by magnetic fields in the plasma.

3.2.2 Luminescent profile screens

A pair of luminescent screens fielded in E1 will measure transverse density modulations in the pair beam.

3.2.3 Heterodyne mixer for sub-mm radiation

A heterodyne mixer will be used to detect the sub-mm wavelength maser emission. This beats the maser signal with a known signal with comparable frequency. A low-pass filter will remove high-frequency components whilst transmitting the beat wave envelope, which is frequency-downshifted with respect to the maser emission. The beat wave envelope is measured electronically, allowing the original maser signal to be retrieved. This detector will be developed in collaboration with Dr. Boon Kok in Astrophysics at Oxford, who has extensive experience with heterodyne detectors for measuring sub-mm wavelength radiation.

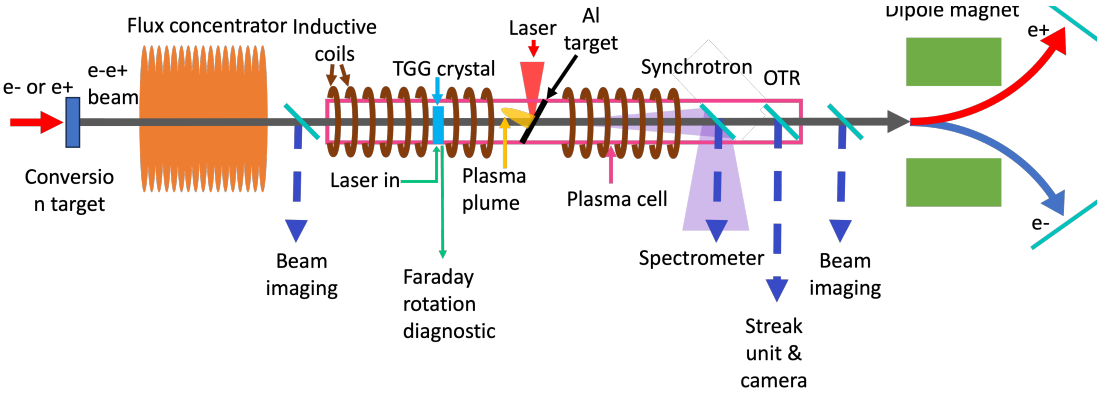

Figure 5: Experimental set-up for particle acceleration measurement. This is similar to the setup for work package E1, with the addition of a nanosecond laser impinging on an Al target. A dipole electromagnet will disperse the electron or positron beam onto one of two luminescent screens either side of the beam axis, enabling spectral retrieval of the accelerated leptons.

3.3 E3: Particle acceleration at relativistic shocks

We plan to study the processes involving relativistic collisionless shocks and particle acceleration. This will provide insight into the mechanisms which are thought to generate energetic cosmic rays, such as Fermi acceleration in relativistic shocks, which have yet to be observed in the laboratory.

This experiment will use the same setup as in E1, but with the addition of a 4.2 J, 6.8 ns Nd:YAG laser with 1064 nm wavelength – see Fig. 5. As discussed earlier, with the plasma densities we will achieve in the experiment, we expect a linear growth rates for the current filamentation instabilities of ≈ 12 e-folding lengths for a 0.1 GeV pair beam with $n_b = 10^9\,\mathrm{cm}^{-3}$ with 25 mrad divergence, propagating though a $2 \times 10^{12}\,\mathrm{cm}^{-3}$ plasma. The flux concentrator can reduce the transverse momentum spread of the pair beam, allowing the beam instability to be investigated for higher plasma densities, up to $10^{14}\,\mathrm{cm}^{-3}$ (this would require beam divergence ≤ 7 mrad). At these plasma and pair beam parameters, the current filamentation instability has a growth rate of $2.3\,\mathrm{ns}^{-1}$, corresponding to ≈ 22 e-folding lengths.

With these e-folding lengths, a collisionless shock is expected to form, and particle acceleration can thus be initiated in the proposed setup. Moreover, in order to assess the importance of upstream turbulence in the energization of particles, we plan to focus the nanosecond laser onto a small Al foil placed inside the plasma cell (see Fig. 5). The laser solid-target interaction will initially produce a $\sim 100\,\mu$m scale solid-density plasma which expands to ~ 1 mm scales over ~ 100 ns [18]. The interaction of the pair beam with this region of higher density plasma will drive a spectrum of plasma waves and kinetic turbulence in the upstream shock. According to numerical simulations shown in Fig. 6 this will significantly enhance particle acceleration. We expect acceleration up to the energy $E_{max} = ecB_{RMS}L \sim 30$ MeV [19], where L is the plasma length, which corresponds to a significant fraction of the beam initial kinetic energy. These energies are readily accessible with the dipole electromagnet we plan to employ in the experiment.

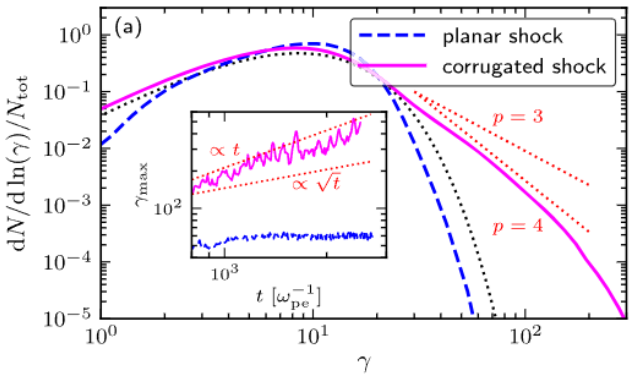

Figure 6: Numerical simulations showing the enhancement of particle acceleration in presence of upstream turbulence. Plot taken from Ref. [13].

4 Costs, Scheduling and Resources

The tasks, timescales and costs associated with the experiments described above are outlined below;

4.1 WP3: Beamline components

- Design, construction and commissioning of the flux concentrator, power supply procurement and installation.
- Spectrometer design, procurement and installation.

Estimated cost; the flux concentrator will cost €600,000.

4.2 WP4: Beam operation

- Dry run to verify beam specifications (charge, energy, emittance, duration etc.) required for the experiment can be delivered by the facility.
- Experiment design, receive equipment shipped from HiRadMat.

WP4.E1 Pair beam instability.

- Develop simulation capabilities to model the spectrum, emission power and longitudinal structure of optical transition radiation emitted by a pair beam interacting with a conducting foil, and the spectrum, emission power and polarisation of synchrotron radiation emitted by the pair beam as it interacts with self-generated magnetic fields in the plasma.
- Further development of the plasma cell and plasma used for a campaign at CERN to reach higher densities $10^{14}\,\mathrm{cm}^{-3}$, and development of a diagnostic capable of measuring such plasma densities. The power supply and matching network used for the CERN experiment can be re-used, which will reduce costs.
- We will field the optical transition radiation diagnostic, synchrotron emission diagnostic and Faraday rotation diagnostic previously used for an experimental campaign at CERN. Additional development may be required to optimise performance of these diagnostics for a campaign at BTF. We have procured a streak unit and camera which can resolve the longitudinal structure of the pair beam, a gated spectrometer suitable for this diagnostic, and a laser, TGG crystal and additional optical components for these diagnostics. In addition to these diagnostics, the beam profile screens and pair spectrometer will need to be designed and requisite components must be procured.
- Experiment installation
- Campaign

WP4.E2 Maser emission

- Development of simulation capabilities to model maser emission.
- Design, development and testing of a heterodyne detector for sub-mm wavelength maser emission.
- Experiment installation
- Campaign

WP4.E3 Particle acceleration

- Simulations must be carried out to identify the conditions requisite for particle acceleration and predict the energy gain of the beam.
- Experiment installation
- Campaign

Estimated cost for the heterodyne detector = €500,000, and for optical elements for diagnostics = €10,000. Plasma cell; if the power supply, matching network from CERN are re-used, a new cell would cost €10,000.

4.3 WP5: Decommissioning

WP5.E1 Radiation safety measures, experiment deconstruction, shipping of diagnostics etc and waste disposal for pair instability experiment.

WP5.E2 Radiation safety measures, experiment deconstruction, shipping of diagnostics etc and waste disposal for maser emission experiment.

WP5.E3 Radiation safety measures, experiment deconstruction, shipping of diagnostics etc and waste disposal for inverse Compton scattering experiment.

Fireball	Year	Year 1												Year 2												Year 3												Year 4						
Task	Month	1	2	3	4	5	6	7	8	9	10	11	12	1	2	3	4	5	6	7	8	8	10	11	12	1	2	3	4	5	6	7	8	9	10	11	12	1	2	3	4	5	6	7
WP3	Beamline components																																											
	Flux concentrator																																											
	Spectrometer magnet																																											
WP4	Beam operation																																											
	Beam dry run																																											
	Experiment design																																											
WP4.E1	Pair beam instability																																											
	Simulations																																											
	Plasma cell development																																											
	Diagnostic development																																											
	Experiment installation																																											
	Campaign																																											
WP4.E2	Maser emission																																											
	Simulations																																											
	Diagnostic development																																											
	Experiment installation																																											
	Campaign																																											
WP4.E3	Particle acceleration																																											
	Simulations																																											
	Experiment installation																																											
	Campaign																																											
WP5	Decommissioning																																											
WP5.E1	Pair beam instability																																											
WP5.E2	Maser emission																																											
WP5.E3	Particle acceleration																																											

Table 1: Gantt chart outlining schedule and tasks for the planned experimental campaigns.

5 Construction Cost

We estimate a the construction cost of the experiment to be €1,120,000. In addition to this, the facility upgrading cost is estimated to be around €2-3 million (including LINAC/BTF operation). This will be better evaluated in the future after the simulation campaign, which should start as soon as possible following positive feedback for the TDR.

References

[1] D. J. Bird, S. C. Corbato, H. Y. Dai, J. W. Elbert, K. D. Green, M. A. Huang, D. B. Kieda, S. Ko, C. G. Larsen, E. C. Loh, M. Z. Luo, M. H. Salamon, J. D. Smith, P. Sokolsky, P. Sommers, J. K. K. Tang, and S. B. Thomas. Detection of a Cosmic Ray with Measured Energy Well beyond the Expected Spectral Cutoff due to Cosmic Microwave Radiation. , 441:144, March 1995.

[2] Tsvi Piran. Gamma-ray bursts and the fireball model. *Physics Reports*, 314(6):575–667, 1999.

[3] Archie F. A. Bott, Petros Tzeferacos, Laura Chen, Charlotte A. J. Palmer, Alexandra Rigby, Anthony R. Bell, Robert Bingham, Andrew Birkel, Carlo Graziani, Dustin H. Froula, Joseph Katz, Michel Koenig, Matthew W. Kunz, Chikang Li, Jena Meinecke, Francesco Miniati, Richard Petrasso, Hye-Sook Park, Bruce A. Remington, Brian Reville, J. Steven Ross, Dongsu Ryu, Dmitri Ryutov, Fredrick H. Séguin, Thomas G. White, Alexander A. Schekochihin, Donald Q. Lamb, and Gianluca Gregori. Time-resolved turbulent dynamo in a laser plasma. *Proceedings of the National Academy of Sciences*, 118(11):e2015729118, 2024/10/28 2021.

[4] A. De Rújula. A cannonball model of cosmic rays. *Nuclear Physics B - Proceedings Supplements*, 151(1):23–32, 2006.

[5] K. I. Kellermann and I. I. K. Pauliny-Toth. The Spectra of Opaque Radio Sources. , 155:L71, February 1969.

[6] Brian D Metzger, Ben Margalit, and Lorenzo Sironi. Fast radio bursts as synchrotron maser emission from decelerating relativistic blast waves. *Monthly Notices of the Royal Astronomical Society*, 485(3):4091–4106, 10/28/2024 2019.

[7] I. Vorgul, B. J. Kellett, R. A. Cairns, R. Bingham, K. Ronald, D. C. Speirs, S. L. McConville, K. M. Gillespie, and A. D. R. Phelps. Cyclotron maser emission: Stars, planets, and laboratory a). *Physics of Plasmas*, 18(5):056501, 10/28/2024 2011.

[8] Mitchell C. Begelman, Robert E. Ergun, and Martin J. Rees. Cyclotron maser emission from blazar jets? *The Astrophysical Journal*, 625(1):51, 2005.

[9] S L McConville, D C Speirs, K Ronald, A D R Phelps, A W Cross, R Bingham, C W Robertson, C G Whyte, W He, K M Gillespie, I Vorgul, R A Cairns, and B J Kellett. Demonstration of auroral radio emission mechanisms by laboratory experiment. *Plasma Physics and Controlled Fusion*, 50(7):074010, 2008.

[10] K. Ronald, D. C. Speirs, S. L. McConville, A. D. R. Phelps, C. W. Robertson, C. G. Whyte, W. He, K. M. Gillespie, A. W. Cross, and R. Bingham. Radio frequency resonator structure and diagnostic measurements for a laboratory simulation of auroral kilometric radiationa). *Physics of Plasmas*, 15(5):056503, 10/28/2024 2008.

[11] Roger Blandford and David Eichler. Particle acceleration at astrophysical shocks: A theory of cosmic ray origin. *Physics Reports*, 154(1):1–75, 1987.

[12] Guy Pelletier, Andrei Bykov, Don Ellison, and Martin Lemoine. Towards understanding the physics of collisionless relativistic shocks. *Space Science Reviews*, 207(1):319–360, 2017.

[13] Camilia Demidem, Joonas Nättilä, and Alexandra Veledina. Relativistic Collisionless Shocks in Inhomogeneous Magnetized Plasmas. *The Astrophysical Journal Letters*, 947(1):L10, 2023.

[14] C. D. Arrowsmith, P. Simon, P. J. Bilbao, A. F. A. Bott, S. Burger, H. Chen, F. D. Cruz, T. Davenne, I. Efthymiopoulos, D. H. Froula, A. Goillot, J. T. Gudmundsson, D. Haberberger, J. W. D. Halliday, T. Hodge, B. T. Huffman, S. Iaquinta, F. Miniati, B. Reville, S. Sarkar, A. A. Schekochihin, L. O. Silva, R. Simpson, V. Stergiou, R. M. G. M. Trines, T. Vieu, N. Charitonidis, R. Bingham, and G. Gregori. Laboratory realization of relativistic pair-plasma beams. *Nature Communications*, 15(1):5029, 2024.

[15] C.D. Arrowsmith, A. Dyson, J.T. Gudmundsson, R. Bingham, and G. Gregori. Inductively-coupled plasma discharge for use in high-energy-density science experiments. *Journal of Instrumentation*, 18(04):P04008, 2023.

[16] N. Vallis, P. Craievich, M. Schär, R. Zennaro, B. Auchmann, H. H. Braun, M. I. Besana, M. Duda, R. Fortunati, H. Garcia-Rodrigues, D. Hauenstein, R. Ischebeck, E. Ismaili, P. Juranić, J. Kosse, A. Magazinik, F. Marcellini, T. Michlmayr, S. Müller, M. Pedrozzi, R. Rotundo, G. L. Orlandi, M. Seidel, N. Strohmaier, and M. Zykova. Proof-of-principle e+ source for future colliders. *Physical Review Accelerators and Beams*, 27(1):013401, 2024.

[17] M. Marongiu, C. Guidorzi, G. Stratta, A. Gomboc, N. Jordana-Mitjans, S. Dichiara, S. Kobayashi, D. Kopač, and C. G. Mundell. Radio data challenge the broadband modelling of GRB 160131A afterglow. *Astronomy & Astrophysics*, 658:A11, 2022.

[18] Yaoxing Wu, Xinbing Wang, Tyler Ray, and Ahmed Hassanein. Experimental study of dynamics and soft x-ray emission of laser produced plasma from low-density foam ti targets. *Vacuum*, 207:111604, 2023.

[19] A M Hillas. The Origin of Ultra-High-Energy Cosmic Rays. *Annual Review of Astronomy and Astrophysics*, 22(1):425–444, 1984.